PAPER REF: 4663

ELASTOPLASTIC MODELLING OF DAMAGE IN POLYMER-CLAY NANOCOMPOSITES WITH EVOLUTIONARY PARTICLE DEBONDING

A.Mesbah[1,2 (*)], F. Zaïri[1], J.M. Gloaguen[3], M. Naït-Abdelaziz[1], K. Azouaoui[2]
[1]Laboratoire de Mécanique de Lille (UMR CNRS 8107), USTL, Polytech'Lille, Avenue P. Langevin, 59655 Villeneuve d'Ascq Cedex, France
[2]Laboratoire de Mécanique Avancée, USTHB, BP32 El-Alia Bab-Ezzouar, 16111 Alger, Algérie
[3]Laboratoire de Structure et Propriétés de l'Etat Solide (UMR CNRS 8008), USTL, Bât. C6, 59655 Villeneuve d'Ascq Cedex, France
(*)*Email:* ammar_mesbah@yahoo.fr

ABSTRACT

Using relationships for nanocomposites based on polymer / clay is of prime importance for the reliable design of these new systems. In this work, we present an analytical model for micromechanical elastoplastic small deformations based on a multi-scale approach wherein the formulation takes into account a third phase corresponding to the disturbance of the polymer matrix located around the nanoparticles. Considering the thickness of the third phase as an internal characteristic dimension, the effect of particle size on the macroscopic behavior is explicitly taken into account in the modeling.

At the microscopic scale, the tensile deformation mechanisms are characterized by a transformation of the microstructure, which can be explained by a simultaneous deformation of the material. However, the process of cavitation by decohesion between clay particles and the polymer matrix (polyamide) were observed in nanocomposites deforming homogeneously in the plastic. In this study, we also present confrontations between the analytical and experimental results obtained from a video-tensile system to measure the true stress-strain and volumetric strain of a sample during a tensile test.

INTRODUCTION

Polymer nanocomposites represent a new alternative to conventionally filled polymers. Because of their nanometer sizes, filler dispersion nanocomposites exhibit markedly improved properties when compared to the pure polymers or their traditional composites. In fact, the interface between nanofiller /polymer an area which represent a significant volume fraction of the nanocomposite, has a major effect on mechanical behavior (Usuki 1993), (Kojima 1993). Very few works deal with the microstructural changes involved during loading in polymer-clay nanocomposites (Gloaguen and Lefebvre, 2001).

Interfacial bonding state is one of the most important factors that control the local fields and overall elastic properties of the nanocomposites (Duan 2007). The imperfect interface term is used to describe a situation in which the displacements are discontinuous between the inclusion and the matrix. They replaced the isotropic debonded inclusions by the perfectly debonded inclusions with transversely isotropic properties to describe the loss of the load-transfer capacity of debonded interface between inclusion and matrix. Models of damage micromechanics for composites considering interfacial debonding have been proposed by

many researchers (Zhao 1997); (Lee 2001); (Liang 2006); (Liu 2006); (Lee 2007). Their approach was derived from the Mori-Tanaka theory based on the modified Eshelby tensor for an inclusion weakened interface proposed by (Qu 1993). Similar work has already been done by (Jun 1997). (Zhong 2004) studied three-dimensional micromechanical modeling of particulate composites with imperfect interface.

To predict the effective plastic yielding response of polymer/clay nanocomposites, (Zaïri 2011) recently proposed a micromechanical model integrating the effects of size and clay structural parameters (i.e. number of clay layers in the nanoparticle and interlayer spacing). The interphase is introduced as a third phase in the mathematical formulation.

The aim of this paper is to extend the model presented by Zaïri taking account consideration the damage mechanisms in the deformation process. Experiments were also achieved to characterize the role of polymer matrix and clay content on the micromechanical deformation processes and the elastic-plastic response. In our approach, three levels of elastic damage model are taken into consideration for a complete description of the sequential progression of a weakened interface in the nanocomposite:

Level 1 status three-phase nanocomposite consisting of a matrix and particles perfectly bonded and interphase around each particle. Level 2 nanocomposites are the four phases are: the matrix, perfectly bonded particles and particles with mildly weakened interface and interphase. Level 3 five-phase state in the nanocomposite comprising a matrix, the particles perfectly bonded, interphase, particles partially debonded and completly debonded particles.

Comparisons between the present prediction with the available experimental data are conducted to better illustrate the behavior of elastic damage of the present framework and verify the validity of proposed multi-level elastic damage model

ELASTOPLSTIC MICROMECHANICAL MODELING

The prediction model elastic presented in this document has been presented in previous works (Mesbah 2009), (Boutaleb 2009) in our group. Therefore, the micromechanical model assumes that the particles are isotropic exfoliated, intercalated particles are assumed transversely isotropic and dispersed in a continuous elastic isotropic medium. The continuous medium is the matrix polymer.

Improvements in mechanical properties of nanocomposites is partly explained by the presence of a region near the stress reinforcement nano (Usuki 1993), (Kojima 1993). The area constraint can be defined as an interphase between the nano-reinforcement and the matrix, due to the interaction between the matrix and local particle. In this work, the area constraint is explicitly taken into account. We assume it has the same form factor as the clay plate. The interfaces between the three phases are considered perfect.

Micromechanics constitutive equations of elasticity can be written as follows:

$$\bar{\mathbf{C}} = \mathbf{C}^M . \left\{ \mathbf{I} - \left(\mathbf{T}^P + \mathbf{T}^I \right) . \left[\left(\mathbf{S}^P . \mathbf{T}^P + \mathbf{S}^I . \mathbf{T}^I \right) + \mathbf{I} \right]^{-1} \right\} \quad (1)$$

$\mathbf{T}^P$ and $\mathbf{T}^I$ **are** two fourth-order tensors expressed as:

$$\mathbf{T}^P = -\phi^P \left[\mathbf{S}^P + \left(\mathbf{C}^P - \mathbf{C}^M \right)^{-1} . \mathbf{C}^M \right]^{-1} \text{ and } \mathbf{T}^I = \phi^I \left[\mathbf{S}^I + \left(\mathbf{C}^I - \mathbf{C}^M \right)^{-1} . \mathbf{C}^M \right]^{-1} \quad (2)$$

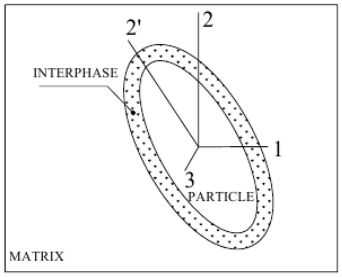

Fig. 1 particle with interphase in space

The clay nanoparticles P surrounded by an interphase I are assumed to have a random orientation and distribution in the polymer matrix M. C^M ,C^P and C^I are the stiffness tensors of the fourth order of the matrix, the particle exfoliated or intercalated and interphase, respectively. $\emptyset^P$ and $\emptyset^I$ define the volume fractions of the particle and the matrix in interphase.

The random orientation of the particles is introduced from the following equation:

$$\langle C_{ijkl} \rangle = \int_0^{\pi} \int_0^{\pi} Q_{mi} Q_{nj} C_{mnpq} Q_{pk} Q_{ql} P(\theta, \emptyset) \sin\theta \; d\theta \; d\emptyset \qquad 3$$

Where $P(\theta, \emptyset)$ is the probability density function and Q_{ij} is the transformation matrix in space.

For simplicity, the von Mises yield criterion with isotropic hardening law is assumed here. Accordingly, at any matrix material point, the stress σ and the equivalent plastic strain e^p must satisfy the following yield function:

$$F\left(\sigma; e_m^p\right) = \sqrt{\sigma : I_d : \sigma} - K\left(\bar{e}_m^p\right) \leq 0 \qquad 4$$

Where $\bar{e}_m^p$ and $K\left(\bar{e}_m^p\right)$, respectively are the equivalente plastic strain and isotropic hardening function of the matrix. In addition, I_d denotes the deviatoric part of the fourth order tensor When a small deformation is considered, the total macroscopic strain $\bar{\varepsilon}$ consists of two parts : $\bar{\varepsilon} = \bar{\varepsilon}^e + \bar{\varepsilon}^p$

$\bar{\boldsymbol{\varepsilon}}^{\boldsymbol{e}}$ denotes the overall elastic strain of the nanocomposites. The relationship between the macroscopic stress $\bar{\sigma}$ and macroscopic elastic strain$\bar{\boldsymbol{\varepsilon}}^{\boldsymbol{e}}$

$$\bar{\sigma} = \bar{C} : \bar{\varepsilon}^e \qquad 5$$

Moreover, $\bar{F}$ is the overall yield function of composites which, based on ensemble homogenization in (Ju, 2001) and the treatment can be micromechanically determined as :

$$\bar{F} = \emptyset^M \sqrt{\bar{\sigma} : \bar{T} : \bar{\sigma}} - K(\bar{e}^p) \leq 0 \qquad 6$$

Were $\emptyset^M$ is volume fraction of matrix

$$K\left(\bar{e}_m^p\right) = \sqrt{\frac{2}{3}\left[\sigma_y + h(\bar{e}^p)^q\right]} \qquad 8$$

The effective yield surface $\bar{F}$ is expressed as a function of the effective equivalent plastic strain $\bar{e}^{\,p}$ as follows (Ju 2001):

$$\bar{F} = \phi^M \sqrt{\frac{3}{2}\langle H \rangle_m} - \sigma_y - h\left(\bar{e}^{\,p}\right)^q \leq 0 \qquad 9$$

in which $\langle H \rangle_m$ is the square of the effective stress. The terms σ_y, h and q denote the initial yield stress, the linear and exponential hardening parameters of the polymer matrix, respectively.

The effective plastic strain rate $\dot{\boldsymbol{\varepsilon}}^{\boldsymbol{p}}$ is given by the normality rule:

$$\dot{\boldsymbol{\varepsilon}}^{p} = \dot{\lambda} \frac{\partial \bar{F}}{\partial \boldsymbol{\sigma}} \qquad 10$$

Where $\dot{\lambda}$ is the plastic multiplier computed from the plastic consistency condition: $\dot{\lambda}\langle \dot{\bar{F}} \rangle = 0$. The yield condition may be formulated in a Kuhn-Tucker form by $\dot{\lambda} \geq 0$, $\langle \bar{F} \rangle \leq 0$, $\dot{\lambda}\langle \bar{\bar{F}} \rangle = 0$.

MATERIALS AND METHODS

In this study, a nanocomposite of polyamide-6 matrix and reinforcing nanoclay montmorillonite type (MMT) was seen with several volume fractions. A Polyamide-6 (PA6) was provided in the form of granulated DSM, Geleen (Netherlands). The reinforcement used is organophilic clay marketed by Southern, known by the name Cloisite. We chose to use the Cloisite© 20A because the surface treatment is adopted in most polymers having a hydrophobic character. The organophilic clay is obtained from natural clay type montmorillonite with cation exchange capacity (CEC) of about. This organophilic clay is obtained from natural clay of the montmorillonite type, having a cation exchange capacity of the order of (92.6meq/100g)

Mixtures of nanocomposites are prepared using a twin-screw extruder which is producing semi-finished or finished products. The design of the screw profile (material transport elements, shearing elements), the number of screws (single-screw, twin-screw), their direction of rotation (corotating or counter) and penetration play a role in the mechanical working provided by (Zhu 2004). The principle of implementation for intercalation extrusion is identical to the case of exfoliated nanocomposites. Two parameters will allow modulating the clay dispersion in the matrix: the extrusion temperature and shear strength in the melt. During extrusion, the temperature between the hopper and the extrusion head is held in 170 and 260 °C for mixtures reinforced polyamide-6 (PA6).

Table 1 Properties of polyamide PA6

Properties	
Melting temperature	**210 to 220°C**
Glass transition temperature	**40 to 60°C**
Young's modulus	**2 GPa**

Three types of nanocomposites reinforced with Cloisite® 20A modified: mass fractions of 2 wt%, 5 wt% and 7.5 wt% were prepared by blending mode in a micro-twin-screw extruder (15 micro DSM), a speed 100 tr/min to 240 °C. The polyamide PA-6 neat has been identified as PA0 the same procedure but without reinforcement. However the test specimens are extruded nanocomposite PA6/20A injection into a metal mold. Before the use of the twin screw extruder, the granules must be dried under vacuum at a temperature of (80°C) for 12 hours before use to prevent degradation reactions induced by moisture. After extrusion, the samples were immediately kept in a vacuum desiccator before use in tests characterizations. The tests were carried on a tensile testing machine electromechanical. The true strain is obtained by analysis of markers placed on the surface of the test specimen.

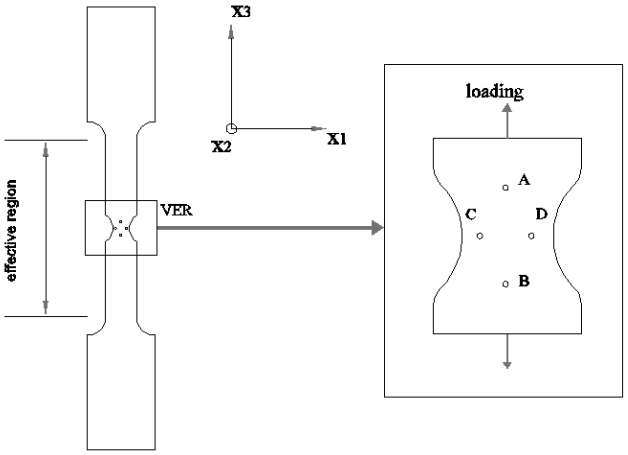

Fig.2 system with four marks on the tensile specimens.

The true stress is defined as the tensile force per unit cross section at markers. Assuming that the strain in the thickness obeys the hypothesis of transverse isotropy (homogeneous distribution of deformation), it is equal to the value measured in the direction of the width.

The system regulates the continuous movement of the cross head of the traction machine according to the instantaneous values of the axial deformation to ensure a constant axial strain rate $(\varepsilon = 5.10^{-4}\ s^{-1})$. The sum of the true strain in the three directions is equal of the total volumic deformation of the material.

The total volumetric strain can be decomposed into two deformations: elastic deformation and plastic deformation induced damage mechanisms. Elastic deformation volumic expressed in terms of Young's modulus and Poisson's ratio is given by: $\varepsilon_v^{el} = (1-2\nu)\frac{\sigma_{33}}{E}$. Plastic volumetric strain is due to the formation, growth and coalescence of cracks. Thus, the plastic volumetric strain can be monitored in real time during the tensile test by the equation: $\varepsilon_v^{pl} = \varepsilon_v - (1-2\nu)\frac{\sigma_{33}}{E}$. The axial true stress σ_{33} (Cauchy stress) takes into account the reduction of the specimen section. We thus obtain the variation the true stress and volumetric strain depending to the true strain. The influence of the rate of nano-reinforcements on the stress-strain curve is shown in Figure 3. The tests were not carried to completion due to the break of the markers. The curves show the typical behavior of large deformation of thermoplastic polymers. A linear elastic phase is immediately followed by nonlinearity to the yield stress and during the phase of plastic deformation, the material is the seat of a hardening associated with the structural orientation. It can also be the seat of a process of damage by decohesion at the interface polymer / nano-reinforcement (Mesbah 2009).

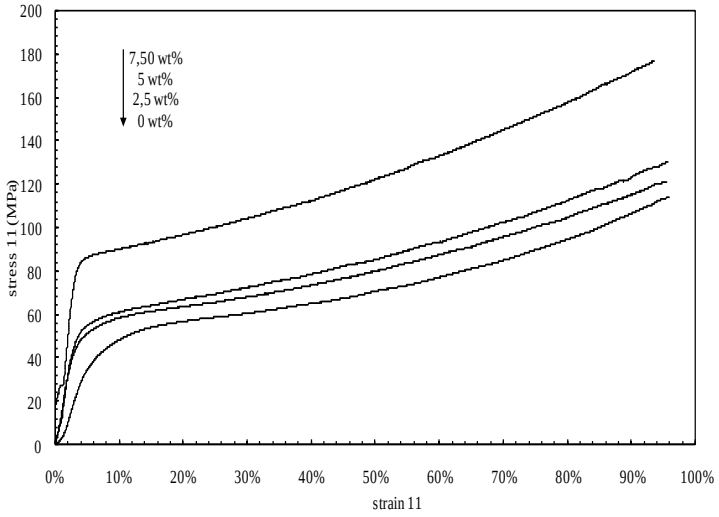

Fig.3 Effect of MMT content on the stress-strain

The influence of nano-reinforcement rate is also shown in this figure. We can see that for nanocomposites small amount of nanoparticles volume variation is negligible. The volumetric strain clear from the elongation controlled by the speed of deformation. When the rate of nano-reinforcements increases, the phenomenon of dilation occurs earlier. In addition, the kinetics of damage, characterized by the slope of the curve is also affected by the quantity of nano-reinforcements.

EFFECTIVE ELASTOPLASTIC BEHAVIOR OF POLYMER MATRIX NANOCOMPOSITES

We now consider the overall elastoplastic responses of progressively debonded silicate-reinforced nanocomposites which initially feature perfect interfacial bonding between particles and the matrix. It is known that partial interfacial debonding may occur in some particles under an applied force. Therefore, initially the nanocomposites are composed of two phases (matrix/reinforcement) and in plastic deformation can gradually become a nanocomposite four-phase: the matrix, perfectly bonded particles, partially debonded and full debonding.

The effective elastic stiffness tensor $\overline{\boldsymbol{C}}$ of the nanocomposite becomes:

$$\bar{C} = C^M.\left\{ I - \left[\sum_1^3 T^{\Sigma_i} \right].\left[\sum_1^3 S^{\Sigma_i} .T^{\Sigma_i} + I \right]^{-1} \right\} \qquad 11$$

in which $\mathbf{T}^{\Sigma_i}$ are fourth-order tensors given by:

$$\mathbf{T}^{\Sigma_i} = \mathbf{T}^{P_i} + \mathbf{T}^{I_i} \qquad 12$$

The terms $\mathbf{T}^{P_i}$ and $\mathbf{T}^{I_i}$ are given by:

$$\mathbf{T}^{P_i} = -\phi^{P_i}\left[\mathbf{S}^{P_i} + \left(\mathbf{C}^{P_i} - \mathbf{C}^M \right)^{-1}.\mathbf{C}^M \right]^{-1} \text{ and } \mathbf{T}^{I_i} = \phi^{I_i}\left[\mathbf{S}^{I_i} + \left(\mathbf{C}^{I_i} - \mathbf{C}^M \right)^{-1}.\mathbf{C}^M \right]^{-1} \qquad 12$$

The total volume fraction of particles ϕ^P is given by:

$$\phi^P = \sum_1^3 \phi^{P_i} \qquad 13$$

C^{P_1}, C^{P_2} and C^{P_3} are the stiffness tensors of the fourth order of the matrix, the particle exfoliated or intercalated and interphase, perfectly bonded particles, partially debonded and completely debonded respectively.

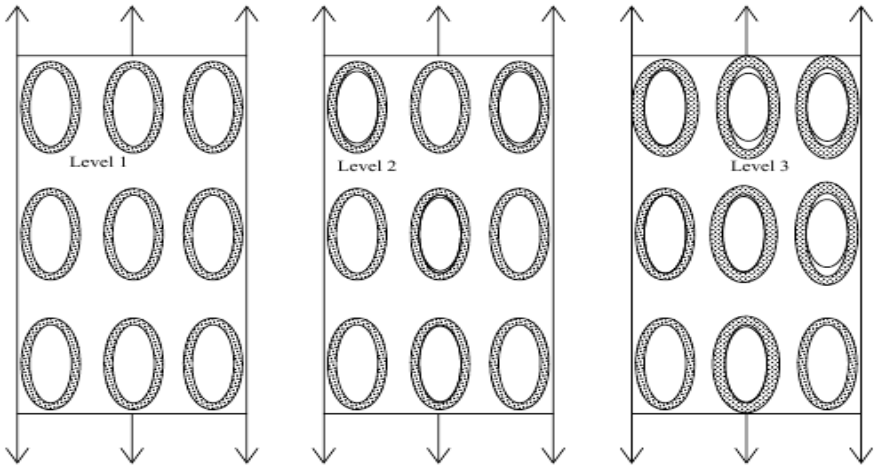

Fig.4 differents levels damage progression of weakened interface in a polymer-clay nanocomposite

PARTICLE DEBONDING EVOLUTION

As loads or deformations increase, resulting in platelet-reinforced nanocomposites increased damage (interfacial debonding) between the particles and the matrix. As a result, the partially debonded particles in the nanocomposites gradually their lose load carrying capacity along the debonded direction. (Zhao 1995), (Ju 2000) and (Ju 2001) proposed a damage model based on the Weibull statistical function to describe the evolutionary interfacial debonding in particle. The internal stress of particles, denoted by σ_p, was chosen to be the controlling factor of the function, and was required for the initiative of the interfacial debonding.

Although micromechanisms interaction between the nanoparticles and the polymer matrix are complicated in nanocomposites, it is clear that the local normal stresses acting on the interface particles are crucial for particle matrix interfacial decohesion. It is also recognized that local shear stresses acting on the particle interface could play a significant role in the interfacial debonding process of composites. However, our approach to the treatment of equivalent particles takes into account only the constraints of the principal directions.

Following the modeling of the elastoplastic behavior of nanocomposites, the average local normal stress on particles is considered a key factor for interfacial debonding, which suggests to assume that the debonding of particles occurs in a certain direction if the normal stress the particle in that direction reaches an intrinsic critical strength bonding of composite materials.

The tensile strength depends on the probability to meet a critical defect and mechanical characterization of damage material requires a statistical approach. The most classic is the Weibull analysis which consists of representing the probability of damage according to level of stress ($\bar{\sigma}_P$) at which the debonding particle.

Two phases in nanocomposite state, in the nonlinear behavior, assuming (Weibull, 1951) statistics governs and some particles with mildly weakened interface are transformed to particles with severely weakened interface when deformations or loads increase. The volume fractions of particles having severely weakened interface($\emptyset^{P_3}$), particles having mildly weakened interface ($\emptyset^{P_2}$) and perfectly bonded particles ($\emptyset^{P_1}$) in the four-phase composite state at a given level of $\bar{\sigma}_P$ can be derived through the following two-step Weibull approach:

$$\emptyset^{P_2+P_3} = \emptyset^{P_2} + \emptyset^{P_3} = \emptyset^{P}\left\{1 - exp\left[-\left(\frac{\bar{\sigma}_P}{s}\right)\right]^m\right\} \quad 14$$

$$\emptyset^{P_3} = (\emptyset^{P_2+P_3})\left\{1 - exp\left[-\left(\frac{\bar{\sigma}_P}{s}\right)\right]^m\right\} \quad 15$$

$$\emptyset^{P_1} = \emptyset^{P} - \emptyset^{P_2+P_3} \quad 16$$

$$\emptyset^{P_2} = \emptyset^{P} - (\emptyset^{P_1} + \emptyset^{P_3}) \quad 17$$

However, the internal stress of the $\bar{\sigma}_P$ particles induced by external loads or deformations and **s** and **m** are the Weibull parameters. The internal stresses of particles required for the initiation of interfacial debonding were explicitly derived by Ju and Lee (1999). For multi-phase composites, the average internal stresses of particles can be expressed as :

$$\bar{\sigma}^{p} = C^{M}.\left\{I - \left[\sum_1^3 T^{\Sigma i} \quad\right].\left[\sum_1^3 S^{\Sigma i} \quad .T^{\Sigma i} \quad + I\right]^{-1}\right\} \quad 18$$

The interfacial debonding is controlled by the average internal stress in the nanoparticle:

RESULTS AND DISCUSSION

To verify the efficiency model capacity to predict the behavior of the nanocomposite, a comparison with experimental results is necessary. In this way, we can both validate our analytical approach one hand and on the other hand make credible our mathematical model. We are interested in this work as elastoplastic modeling nanocomposites. Young's modulus and Poisson's ratio of nanoclay are taken equal to 178 GPa and 0.23, respectively. If the thickness of a sheet is known to be approximately equal to 1 nm, its length is not constant and varies between 100 and 500 nm (Sheng 2004).

The analytical predictions are compared with experimental characteristics reported in the literature. These nanocomposites are silicates montmorillonite (MMT) dispersed in a polymer matrix, which is considered fully exfoliated.

To enhance our analytical model confrontation with experimental results related by (Rajinder 2008) for nanocomposites of polyamide / clay are considered. The analytical predictions consider the particles with a unidirectional orientation in the nanocomposite but a overestimation is observed compared with the experimental results. Only the predictions of nanocomposite with particles random orientation provide assessments acceptable.

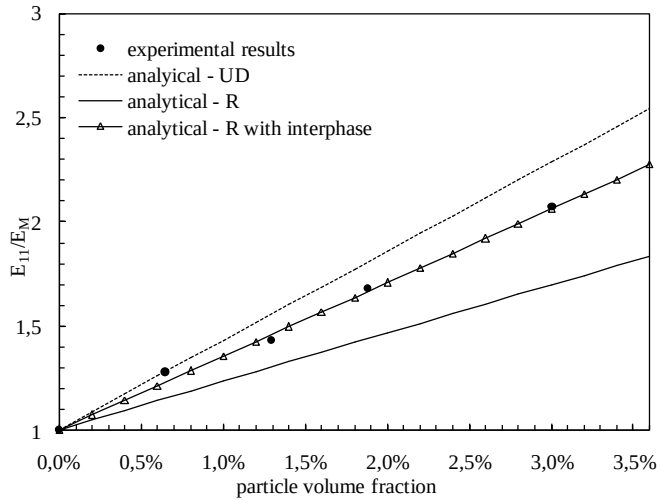

Fig.5 Comparison between analytical prediction and experimental results of Young's modulus of nanocomposites overall (polyamide / clay) (Rajinder 2008)

(UD unidirectional particle orientation, R, randomly oriented particles)

In Fig.5, the predictions are very good in the concordance of all volume fractions and the influence of a constraint region (interphase) is taken into account. Since there is no mechanical characteristic about this interphase, a Young's modulus and Poisson's ratio of 0.4 were assigned. The volume fraction of the interphase in the middle of full inclusion was set at 25%. As shown in Figure the presence of interphase effects on stiffness.

The proposed multi-damage model is further exercised to predict the behavior of polymère/nanoclay nanocomposites. The uniaxial stress–strain behavior of randomly oriented particles, takes into account the structural morphologie from intercalated and exfoliation. It has been shown that the composites are quasi-isotropic. Fig.6 and Fig.7 shows typical traction curves of the neat matrix and the nanocompsites (nanoclay/PA6) with three differents volumes fractions. The linear part corresponds to the elastic behavior. The deviation from linearity coincides with the occurrence of the plastic deformation and damage is initiated.

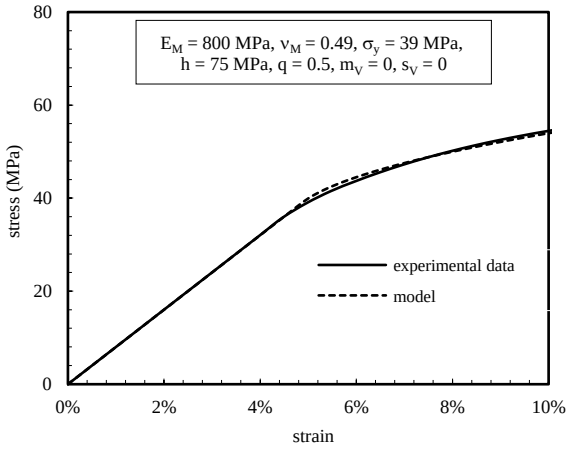

Fig.6. Comparison between model and experimental data of neat polyamide-6

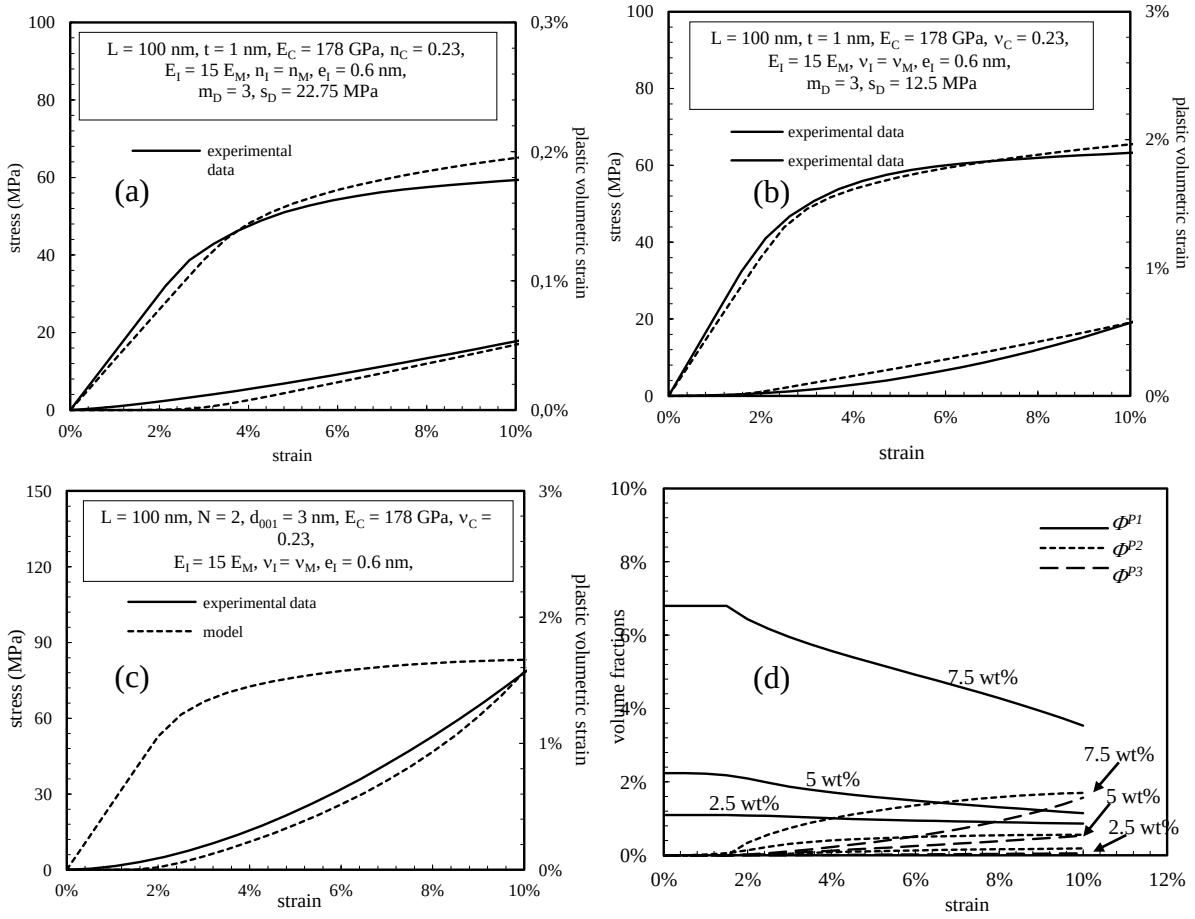

Fig.7. Comparison between micromechanical model and experimental data of polyamide-6 filled with (a) 2.5 wt%, (b) 5 wt%, (c) 7.5 wt% of MMT clay and (c) evolution with strain of volume fractions.

In Fig.6, true axial stress and true plastic volumetric strain are plotted versus true axial strain for the neat polyamide-6. In this section, we are only focused on experimental data given by solid lines. This matrice may be regarded as model one. Indeed, the polyamide-6 matrix deforms exclusively by shear. The uniaxial tensile tests provide important indications concerning the macroscopic response and the micromechanisms of damage involved in polymer-clay nanocomposite systems. The origin of the reduction slope comes from the debonding of the interface particle /matrix. When the interfacial stress becomes higher than the resistance of the interphase particle / matrix, the latter breaks and the decohesion propagates along the interface. It should be noted that, due to stress concentrations generated by the inclusion of a particle rigidity different from its surroundings, the stress of debonding is not strictly equal to the applied stress on the material. When debonding is complete, the particle is no longer bound to the matrix and the effective area supporting the external forces is reduced simply to the matrix Fig.7.

In Figs.7 (a, b and c), true axial stress and true plastic volumetric strain are plotted versus true axial strain for polyamide-6-clay nanocomposites. A significant influence of clay content on the plastic volumetric strain is pointed out for nanocomposites. When the clay loading increases the dilatational mechanisms constitute an important part of the apparent deformation. Figures show the predictions of the stress-strain response of nanocomposites PA6/20A with weakened interfaces under uniaxial loading and hydrostatic tension. Also show

the evolution of the interfacial debonding with particles as functions of the axial strain and hydrostatic corresponding to a faster evolution of the partial separation and lower stress-strain response**.** Fig.7 shows predictions the evolution of volume fractions of perfectly bonded particles, particles with mildly weakened interface, and particles with severely weakened interface, respectively, as a function of uniaxial strain corresponding to fig.7 d. As a whole, the present prediction and the experimental data match well.

CONCLUSION

We have highlighted the interest of organophilic montmorillonites as nanorenfort in a polyamide matrix. Exfoliation or montmorillonite intercalation results from the coupling between the physical chemistry of interactions polyamide/ Cloisite 20A and the shear provided by the mixing tool, the twin screw extruder. The interaction between the clay and the matrix was explicitly introduced in a micromechanical model assuming the presence of an interphase (region constraint) between the matrix and the nanoparticle. Taking the thickness of the interphase as a characteristic length internal to predict the elastic stiffness of the nanocomposites. It has been shown that even if the clay content is the dominant parameter stiffening, the contribution of the interphase is not negligible.

The micromechanical model of elastic damage is applied to the uniaxial tension loading to predict stress–strain responses. A parametric analysis is also carried to address the influence of the compliance and Weibull parameters on the progressive weakened interface between particles-matrix. Finally, the present predictions are compared with experimental data to further illustrate the elastic damage behavior of the present framework and to verify the validity of the proposed multi-level elastic damage model. Search result shows the effect of elastic expansion at the beginning of the solicitation. When the volume fraction of nano-reinforcements increases the expansion phenomenon is promoted. The predicted stress–strain behavior of particulate composites featuring the multi-level damage progression of weakened interface is observed to be in good qualitative agreement with experimental data.

The model will be extended in addition to the particle matrix decohesion, the void in the matrix due to plastic deformation will be incorporated into the present framework and the corresponding computational algorithm will be systematically developed.

REFERENCES

Boutaleb S., Zaïri F., Mesbah A., Naït-Abdelaziz M., Gloaguen J.M., Boukharouba T., Lefebvre J.M., Micromechanics-based modelling of stiffness and yield stress for silica/polymer nanocomposites, Inter. J. Solids Struct. 2009, 46, 1716-1726.

Duan, H.L., Yi, X., Huang, Z.P., Wang, J. A unified scheme for prediction of effective moduli of multiphase composites with interface effects. Part I: theoretical framework. Mechanics of Materials, 2007, 39, 81–93.

Gloaguen J.M., Lefebvre J.M., Plastic deformation behaviour of thermoplasstic/clay nanocomposites, Polymer. 2001, 42, 5841-5847.

Haian, L. The validity of the modified Mori-Tanaka method for composites with slightly weakened interface. Acta Mechanica Solida Sinica. 1997,10 (2), 108–117.

H.K.. A computational approach to the investigation of impact damage evolution in discontinuously reinforced fiber composites. Computational Mechanics. 2001, 27, 504–512.

Ju JW, Sun LZ. Effective elastoplastic behavior of metal matrix composites containing randomly located aligned spheroidal inhomogeneities. Part I: micromechanics-based formulation. Inter J Solids Struct 2001, 38, 183-201.

Kojima Y., Usuki A., Kawasumi M., Okada A., Fukushima Y., Kurauchi T., Kamigaito O. Mechanical properties of nylon 6-clay hybrid, J. Mater. Res. 1993, 8, 1185-1189.

Lee, H.K. A micromechanical damage model for effective elastoplastic behavior of ductile matrix composites considering evolutionary complete particle debonding. J. Comput. Meth. Appl. Mech. Engng., in press. 1999

L. Zhu, M. Xanthos, Effects of processing conditions and mixing protocols on structure of extruded polypropylene nanocomposite, J. Appl. Polym. Sci., 2004, 93, p. 1891-1899

Liang, Z., Lee, H.K., Suaris, W. Micromechanics-based constitutive modeling for unidirectional laminated composites. International Journal of Solids and Structures. 2006, 43, 5674–5689

Liu, H.T., Sun, L.Z., Ju, J.W. Elastoplastic modeling of progressive interfacial debonding for particle-reinforced metal matrix composites. Acta Mechanica. 2006, 181, 1–17.

Lee, H.K., Kim, B.R. Numerical characterization of compressive response and damage evolution in laminated plates containing a cutout. Composites Science and Technology, 2007, 67, 2221–2230.

Mesbah A., Zaïri F., Boutaleb S., Gloaguen J.M., Naït-Abdelaziz M., Xie S., Boukharouba T., Lefebvre J.M., Experimental characterization and modeling stiffness of polymer/clay nanocomposites within a hierarchical multiscale framework, J. Appl. Polym. Sci. 2009,114, 3274-3291.

N. Sheng, M.C. Boyce, D.M. Parks, G.C. Rutledge, J.I. Abes, R.E. Cohen, Multiscale micromechanical modeling of polymer/clay nanocompositesand the effective clay particle, Polymer 45 (2004) 487-506

Rajinder Pal, Mechanical properties of composites of randomly oriented platelets, Composites: Part A 39 (2008) 1496–1502

Qu, J. The effect of slightly weakened interfaces on the overall elastic properties of composite materials. Mechanics of Materials. 1993, 14, 269–281.

Usuki A., Kojima Y., Kawasumi M., Okada A., Fukushima Y., Kurauchi T., Kamigaito O. Synthesis of nylon 6-clay hybrid, J. Mater. Res. 1993, 8, 1179-1184.

Weibull W. A statistical distribution function of wide applicability. J Appl Mech 1951, 18, 293–297.

Zaïri F, Gloaguen JM, Naït-Abdelaziz M, Mesbah A, Lefebvre JM. Study of the effect of size and clay structural parameters on the yield and post-yield response of polymer/clay nanocomposites via a multiscale micromechanical modelling. Acta Mater 2011, 59, 3851-63.

Zhao, Y.H., Weng, G.J.,. Transversely isotropic moduli of two partially debonded composites. International Journal of Solids and Structures. 1997, 34, 493–507.

Zhong, Z., Yu, X.B., Meguid, S.A. 3D micromechanical modeling of particulate composite materials with imperfect interface. International Journal of Multiscale Computational Engineering, 2004, 42, 172–187.